Break-junction experiments on URu2Si2 single crystals

Naidyuk, Y.G.; Gloos, K.; Menovsky, A.A.

DOI
10.1088/0953-8984/9/31/001
Publication date
1997

Published in
Journal of Physics-Condensed Matter

J. Phys.: Condens. Matter **9** (1997) 6279–6291. Printed in the UK PII: S0953-8984(97)80606-6

Break-junction experiments on URu_2Si_2 single crystals: from bulk transport to vacuum tunnelling

Yu G Naidyuk†‡, K Gloos† and A A Menovsky§

† Institut für Festkörperphysik, Technische Hochschule Darmstadt, D-64289 Darmstadt, Germany

‡ Verkin Institute for Low Temperature Physics and Engineering, National Academy of Science of the Ukraine, 310164 Kharkiv, Ukraine

§ Van der Waals–Zeeman Laboratorium, Universiteit van Amsterdam, 1018 XE Amsterdam, The Netherlands

Received 3 January 1997, in final form 18 April 1997

Abstract. Mechanically controllable break junctions of the heavy-fermion superconductor URu_2Si_2 have been investigated. Josephson-like I–V characteristics could be found only for low-ohmic contacts, but without the oscillatory pattern of the critical current in a magnetic field. High-ohmic contacts always had a finite residual resistance as if there was a normal layer at the contact. *Some* of these contacts showed Andreev-reflection-like features in the differential resistance $\mathrm{d}V/\mathrm{d}I(V)$, while resistive transport *usually* affected them. We have also realized true vacuum tunnelling: the exponential dependence of the current on the width of the vacuum gap and the transition from tunnelling to metallic contact indicate a nearly free-electron mass of the tunnelling charge carriers, as well as a typical metallic carrier density of URu_2Si_2. The temperature dependence of the tunnelling current yields direct information about the thermal-expansion coefficient of the URu_2Si_2 samples and its anisotropy. The superconducting features of the I–V characteristic vanish when the contact resistance exceeds about 1 kΩ. They could not be resolved by vacuum tunnelling, pointing to a pair-breaking effect of the heavy-fermion interfaces.

1. Introduction

The nature of the superconducting (SC) ground state of the heavy-fermion (HF) compounds has been under investigation since the discovery of the first HF superconductor about 17 years ago; see [1] and references therein. The main question still to be resolved is that of the symmetry of the SC order parameter, which is commonly believed to be strongly anisotropic. Tunnelling and point-contact spectroscopy are direct methods for determining the spatial dependence of the amplitude and the phase of the SC order parameter [2, 3]. Unfortunately, both methods are very sensitive to the surface condition. Notable difficulties are the contamination of the surface, for example by oxide, and mechanical stress. We tried to combine and to improve the above two methods using mechanically controllable break junctions (MCB), a technique developed by Muller *et al* [4]. MCB make it possible to prepare clean surfaces and interfaces '*in situ*' at low temperatures and under ultra-high-vacuum conditions, to finely control the contact resistance over many orders of magnitude, and to measure I–V characteristics from low-ohmic metallic contacts to high-resistance tunnel junctions.

Our investigation concentrates on the HF compound URu_2Si_2. The power law for its heat capacity below T_c [5], for example, indicates a strong anisotropy of the SC energy

0953-8984/97/296279+13$19.50

gap, and probably an unconventional SC ground state. Our aim was to prepare Josephson contacts to investigate the microscopic coherence of the SC wave function across the MCB constriction. But the Josephson coupling was found to be suppressed even between two pieces of the same URu_2Si_2 sample, i.e. at a symmetrical homocontact. The SC features of the I–V characteristic vanish with increasing MCB resistance, and they can no longer be resolved in the vacuum-tunnelling regime. Despite these disappointing results, we show that the MCB technique can yield valuable information both on the SC and the normal ground state of URu_2Si_2. We found the coexistence of SC and magnetic features in the $dV/dI(V)$ dependences. From tunnel experiments, we derive several electronic properties of URu_2Si_2, and the temperature dependence of the thermal-expansion coefficient at low temperatures. This investigation also points to further lines of inquiry: the transition between the tunnelling and the metallic regime; the search for Andreev and multiple Andreev reflections; or the critical transport properties in the constricted geometry for the HF superconductor.

2. Experimental details

Our experimental set-up [6, 7] is similar to that described by Muller *et al* [4, 8]. The samples were cut into 3–5 mm long slabs of about 1×1 mm^2 cross section, and glued—electrically isolated—onto a gold-plated copper–bronze bending beam 0.5 mm thick. A spark-cut nut $\sim$0.6 mm deep defines the break position. A screw, driven by two thin (0.3 mm diameter) cotton threads, breaks the sample at low temperatures, and makes the coarse adjustment. The vertical resolution is about 1 μm. A piezo-tube serves for fine adjustment, with 10 pm resolution at low temperatures. The vertical motion of the piezo-tube is transferred to a horizontal displacement of the two parts of the sample against each other, reduced by a factor of order 100. This results in an excellent mechanical stability of the MCB. The device sits in the vacuum region of the refrigerator. A magnetic field could be applied perpendicular to the contact axis; the residual field was less than about 0.1 mT. $R(V) = dV/dI(V)$ as well as $R(T)$ for the metallic contacts were measured with the standard current-biased four-terminal lock-in detection technique. In the tunnelling regime the MCB was biased and the current detected using an electrometer.

We checked the apparatus on break junctions of aluminium. For normal-state contacts with values of R_N up to $\approx$100 Ω the residual resistance was $R = 0$ Ω for $T \to 0$. The width $4\Delta = 0.7$ meV of the SC anomalies, for both metallic and vacuum-tunnelling contacts, demonstrates that our experiments are not limited by electrical noise.

The brittle HF single crystals crack into two pieces with almost mirror-like flat opposite faces, quite unlike the soft Al. The first complete fracture of URu_2Si_2 MCB to infinite resistance occurs at $R_{crit} \simeq$ 1–10 Ω. After each readjustment of the junction, R_{crit} increases, allowing us to prepare metallic contacts up to a few kΩ. In the tunnelling regime we could vary the MCB resistance continuously from a few GΩ down to several tens of kΩ using the piezo-tube.

Here we present the results for five URu_2Si_2 single crystals: two pieces were cut in the c-direction from batch No 338, and one slab in the a-direction and two slabs in the c-direction from batch No XY. $R(T)$ just before breaking indicates a residual resistivity of about 20 $\mu\Omega$ cm at $T \approx$ 1.5–2.0 K. The critical temperature $T_{c,PC}$ defined as the midpoint of the SC transition in $R(T)$ was 1.2 K for batch No 338 and 1.4 K for batch No XY. Thermal-expansion measurements sensitive to the bulk critical temperature (see below) also indicate a larger critical temperature for the batch No XY. Nevertheless, the different sample quality had no influence on the main issue of the paper.

3. Theoretical background

The basic characteristic of a point contact (PC) is its lateral size. The small size restricts the electron flow, and results in a potential drop near the orifice, and an additional contact resistance. The general formula for describing the PC resistance for arbitrary electronic mean free path l and PC diameter d was derived by Wexler [9]. It is approximately the sum of the ballistic Sharvin ($l \gg d$) resistance and the diffusive Maxwell ($l \ll d$) resistance:

$$R_{PC}(T) \simeq \frac{16\rho l}{3\pi d^2} + \frac{\rho(T)}{d} \tag{1}$$

with $\rho l = p_F/ne^2$, where ρ is the electrical resistivity, p_F the Fermi momentum, n the density of electrons, and e the electron charge. The first term of equation (1) corresponds to the ballistic transport of electrons through the constriction, depending on the cross-sectional area. The second term describes diffusive or thermal electron flow in the PC, similar to electron transport in the bulk. Whether the Sharvin or the Maxwell term dominates depends on the relationship between d and ρ. For high-resistivity samples and large contacts, Maxwell's contribution plays the dominant role, while for clean metals and small constrictions, Sharvin's term dominates. From $R_{PC}(T)$ one can determine the contact diameter d, using [10]

$$d = \frac{\mathrm{d}R_{PC}/\mathrm{d}T}{\mathrm{d}\rho/\mathrm{d}T} \qquad T > T_c \tag{2}$$

independently of the residual resistance.

For superconductor–constriction–normal-metal (S–c–N) contacts the contribution from Maxwell's term in the superconducting electrode vanishes because $\rho = 0$, while the ballistic resistance can decrease by as much as a factor of two as a result of Andreev reflection at the N–S boundary [3]. Blonder, Tinkham and Klapwijk (BTK) derived the I–V characteristic for ballistic S–c–N contacts [3]:

$$I(V) \sim \int_{-\infty}^{\infty} T(E)\{f(E - eV) - f(E)\} \qquad \mathrm{d}E \tag{3}$$

$$T(E) = \begin{cases} \dfrac{2\Delta^2}{E^2 + (\Delta^2 - E^2)(2Z^2+1)^2} & |E| < \Delta \\ \dfrac{2|E|}{|E| + \sqrt{(E^2 - \Delta^2)}(2Z^2+1)} & |E| > \Delta. \end{cases}$$

Here $f(E)$ is the Fermi distribution function, Δ the SC energy gap, and Z the strength of the barrier at the interface. The finite quasiparticle lifetime τ in the superconductor broadens the quasiparticle density of states

$$N(E, \Gamma) = \mathrm{Re}\left\{\frac{E - \mathrm{i}\Gamma}{\sqrt{(E - \mathrm{i}\Gamma)^2 - \Delta^2}}\right\}$$

and is taken into account by the modified BTK theory [11]. Here $\Gamma = \hbar/\tau$ is the broadening parameter.

The most interesting feature of S–c–S contacts is the Josephson supercurrent, with critical values of $I_c \simeq (2\text{–}3)\Delta_0/R_N$ [12] for dirty and clean contacts, respectively. An unambiguous test for this Josephson current is observing a Fraunhofer-type diffraction pattern in a magnetic field B:

$$I_c(B) = I_c(0)\left|\frac{\sin(\pi\Phi/\Phi_0)}{(\pi\Phi/\Phi_0)}\right|$$

with $\Phi_0 = h/2e = 2.07 \times 10^{-15}$ T m^2, and $\Phi \propto B$, the magnetic flux in the plane of the contact. Contrary to the case for junctions with conventional superconductors, for Josephson contacts between conventional and unconventional superconductors, critical-current oscillations are expected with a minimum at $B = 0$ instead of a maximum [13]. This can be used as a direct test for the symmetry of the SC ground state.

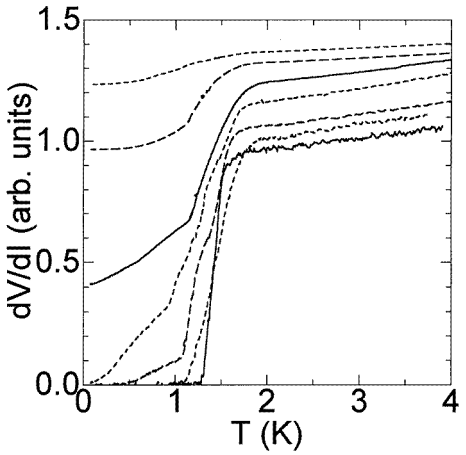

Figure 1. The differential contact resistance $R = \mathrm{d}V/\mathrm{d}I$ at zero bias versus temperature T for URu_2Si_2 MCB along the c-direction. The resistance in the normal state at $T \simeq 2$ K was (from top to bottom) 136, 10, 0.64, 1.4, 0.1, 0.03, and 0.003 Ω, respectively.

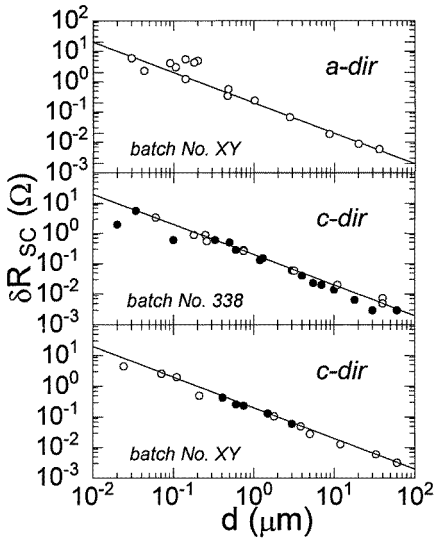

Figure 2. The resistance drop δR_{SC} versus the diameter d of URu_2Si_2 MCB for the two main crystallographic directions. Different symbols correspond to different samples. The solid lines represent $\delta R_{SC} = \rho_{SC}/d$ with $\rho_{SC} = 20$ $\mu\Omega$ cm.

4. Results

4.1. Low-ohmic contacts

For contacts with normal-state resistances ranging from a few mΩ to several Ω, we found that the resistance can vanish below the SC critical temperature T_c (figure 1). With increasing PC resistance, the SC transition in $R_{PC}(T)$ broadens. From $R_{PC}(T)$ at $T > T_c$ we calculate the diameter d of the contacts, by applying equation (2), and we determine the reduction δR_{SC} of the PC resistance due to superconductivity, as described in reference [14].

We have found, in agreement with recent MCB experiments on other HF superconductors [6], that δR_{SC} scales inversely with the PC diameter like Maxwell's resistance, $\delta R_{SC} \simeq \rho_{PC}/d$ (figure 2), and $\rho_{PC} \simeq 20$ $\mu\Omega$ cm as in the bulk [5]. This means that transport processes in PC described by the specific resistivity play an important role. They have to be taken into account for high-resistance MCB before speculating about other spectroscopic features of the $\mathrm{d}V/\mathrm{d}I$ curves connected with ballistic transport.

I–V characteristics of those low-ohmic contacts can show a Josephson-like behaviour with zero resistance up to a critical current I_c. To find the oscillations of I_c we measured $\mathrm{d}V/\mathrm{d}I$ and V at constant bias current I near I_c, while slowly sweeping the magnetic field. This was done for PC with sufficiently large resistances R_N and small currents I_c.

Otherwise, the whole set-up would heat up, because of the power generated in the contacts of the current leads and in the junction itself.

For example, one contact had $R_N \simeq 0.25\ \Omega$, $d \simeq 0.7\ \mu$m, and $I_c(B = 0) \simeq 1.8$ mA. Assuming a magnetic penetration depth of $\lambda \simeq 0.7\ \mu$m [1], the beat period is expected to be $\delta B \simeq \Phi_0/\lambda d \simeq 4$ mT. However, no such oscillations could be found in the field range ± 9 mT, although the product $I_c R_N \simeq 450\ \mu$V almost equalled the Kulik–Omelyanchouk (KO) [12] value $I_c R_N \simeq 2\Delta_0 \simeq 3.52\, k_B T_c \simeq 400\ \mu$V for dirty S–c–S contacts. Note that the KO theory is valid only for $d \ll \xi$, which is not fulfilled for our contacts due to the small SC coherence length $\xi \simeq 10$ nm of URu_2Si_2 [1].

The critical current density of these contacts is of order 10^5 A cm^{-2}, two orders of magnitude smaller than for Al break junctions [7]. The above contact was driven normal only at much higher fields, around 0.3 T. Therefore we believe that I_c for a URu_2Si_2 junction represents mainly the critical current of the resistive transport through the PC caused by ρ being zero, and I_c contains only a very small contribution from the coherent coupling of the SC condensate.

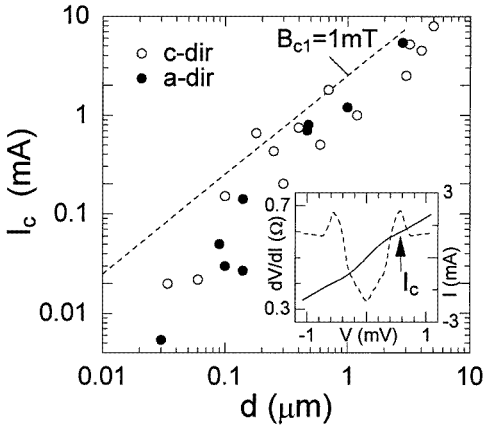

Figure 3. The critical current I_c versus the PC diameter d at $T \leqslant 0.1$ K for URu_2Si_2 MCB in the two crystallographic directions. The dashed line shows $I = (\pi B/\mu_0)d$ with $B = B_{c1} \simeq 1$ mT. The inset shows how I_c is defined.

Three URu_2Si_2 samples out of five had a finite residual resistance already, before breaking them, probably because of intrinsic cracks. Here we define as the critical current I_c the value at which the differential resistance has a peak (see the inset of figure 3). Figure 3 shows I_c versus the PC diameter, as well as the current $I = (\pi B/\mu_0)d$ at which the self-magnetic field B equals $B_{c1} \simeq 1$ mT [1]. When this field exceeds B_{c1}, it could drive the contact region into the mixed state [15], with an $I_c(T) \propto B(T)$ dependence between those of the bulk and the lower critical field (figure 4(a)).

4.2. Typical metallic point contacts

Contacts with normal-state resistance between a few ohms and a few hundred ohms always had a finite residual resistance. Usually their $\mathrm{d}V/\mathrm{d}I(V)$ characteristics had a V-like shape around $V = 0$ (see the inset of figure 3), and more or less pronounced maxima at $V_c = \pm(0.35$–$0.5)$ mV. These maxima shift to slightly higher values at larger PC resistances. The relative size of the SC features becomes smaller with increasing PC resistance, but they

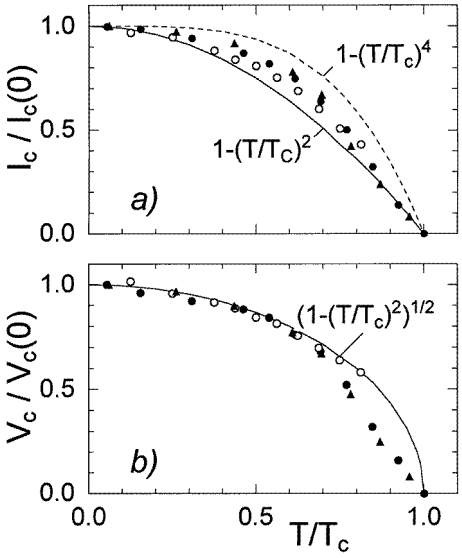

Figure 4. (a) The reduced critical current $I_c/I_c(0)$ versus the reduced temperature T/T_c. Solid and dashed lines display the temperature dependences of the bulk $B_c \sim 1-(T/T_c)^2$ and the lower critical field $B_{c1} \sim \lambda^{-2} \sim 1-(T/T_c)^4$, respectively [18]. (b) The reduced critical voltage $V_c/V_c(0)$ versus the reduced temperature T/T_c. The dashed line corresponds to equation (4). Here T_c is the temperature at which the SC features vanish.

are still resolvable for some PC up to 1 kΩ. Our earlier experiments on heterocontacts [16] showed the SC features disappearing already at resistances of 10 Ω. Obviously the break junctions have considerably improved interfaces.

Several PC with resistances between 20 and 130 Ω had U-shaped characteristics around $V = 0$ and sharp maxima at $V_c \approx \pm 0.35$ mV (figure 5(a)). The position of the maxima corresponds to $eV_c = 3.63\,k_B T_{c,PC}$ [17], describing local heating of the PC due to the bias voltage. Figure 5(c) shows the temperature dependence of V_c following perfectly the behaviour expected for the thermal regime $d \ll l_e$ [17] (l_e is the inelastic mean free path of the electrons):

$$V_c = 2\sqrt{L(T_{c,PC}^2 - T^2)} \tag{4}$$

where $L \simeq L_0 = 2.45 \times 10^{-8}$ V^2 K^{-2} is the Lorenz number. Assuming $V_c \propto T_{c,PC}$ at $T \ll T_{c,PC}$, the magnetic field dependence of V_c (figure 5(d)) is $V_c/V_c(0) \simeq (1 - B/B_c)^{1/2}$, as expected from the phenomenological temperature dependence $B_c = B(0)(1-(T/T_c)^2)$ (reference [18]).

At higher bias, $\mathrm{d}V/\mathrm{d}I$ increases, and shows at $V = \pm$(7–8) mV an N-shaped feature (figure 5(b)), corresponding to the transition into the paramagnetic state above the Néel temperature $T_N \simeq 17.5$ K, similar to the $\rho(T)$ dependence [5]. These characteristics also obey perfectly the thermal limit of PC spectroscopy. When the voltage is increased, superconductivity is suppressed, due to the increased temperature in the PC, to above $T_{c,PC}$; this is followed by the destruction of the antiferromagnetic state when T_N is exceeded at still higher voltages.

The same heating process could be responsible for the shape of $\mathrm{d}V/\mathrm{d}I$ for our other PC with a V-shaped dependence around $V = 0$. But from these characteristics, it was difficult

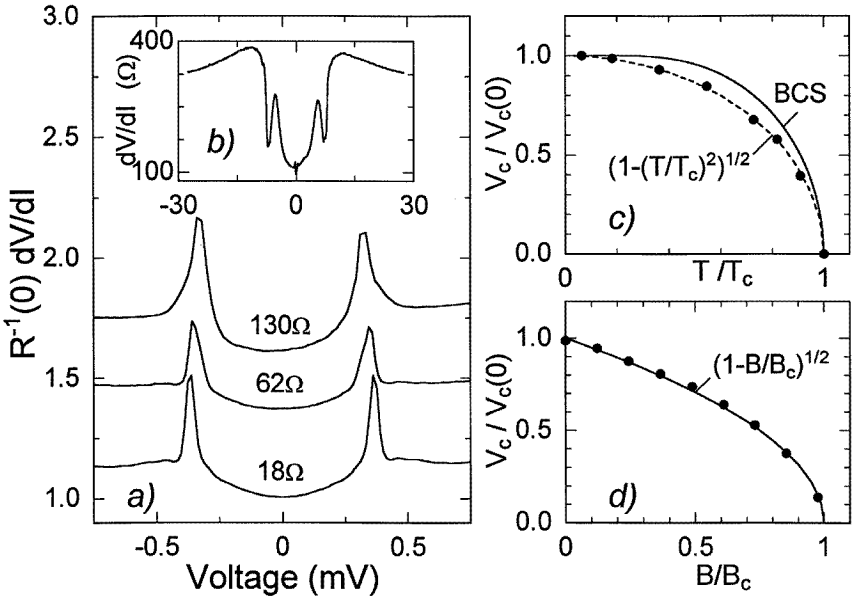

Figure 5. (a) The reduced differential contact resistance $\mathrm{d}V/\mathrm{d}I(V)$ versus the voltage V along the a-direction of three PC with U-shaped characteristics at $T \leqslant 0.1$ K. (b) The differential contact resistance versus the voltage on a larger voltage scale at $T \leqslant 0.1$ K. (c) The position V_c of the maximum of $\mathrm{d}V/\mathrm{d}I$ versus the reduced temperature T/T_c for the PC with $R(0) = 18\ \Omega$ of figure 5(a) ($B = 0$, $T_c \simeq 1.1$ K). (d) V_c versus the reduced magnetic field B/B_c at $T \leqslant 0.1$ K ($B_c \simeq 4.5$ T). Here T_c is the temperature at which the SC maxima vanish.

to determine V_c, because the maxima were less pronounced, and they were broadened near $T_{c,PC}$. Nevertheless, $V_c(T)$ also follows equation (4) quite well, at least below $T \leqslant 0.8T_c$ (figure 4(b)). This broadening, as well as the V shape at $V = 0$, could result from a distribution of critical temperatures in the PC that can also broaden the $R_{PC}(T)$ transition (figure 1) of high-resistance contacts.

The third type of $\mathrm{d}V/\mathrm{d}I$ characteristic shows a small maximum at $V = 0$—that is, a double-minimum structure (figure 6, inset). This feature appeared more often at contacts along the ab-plane than along the c-axis, which also had structures about twice as broad. Similar anisotropies of the $\mathrm{d}V/\mathrm{d}I$ characteristics were found previously with heterocontacts [19].

The double-minimum structure is usually viewed as a characteristic of Andreev reflection (AR) at an N–S interface with quasiparticle reflection, described by the Z-parameter [3]. The finite residual resistance of most of our URu_2Si_2 MCB indicates such a normal layer in the contact; thus the AR process can take place. The maxima at higher voltages shifted with increasing R_{PC}. They are therefore very probably related not to any spectroscopic features, but to the destruction of superconductivity by local heating. The contribution of AR may be resolved at low bias, when local heating is negligible.

A quite different mechanism for producing zero-bias maxima is Kondo scattering, as recently studied on MCB of classical Kondo alloys [20]. For our contacts this could be explained by a small number of disordered uranium ions. A description in terms of non-interacting magnetic impurities seems to be reasonable. We have applied both models to $\mathrm{d}V/\mathrm{d}I(V)$ at low bias: the modified BTK theory was fitted according to equation (3),

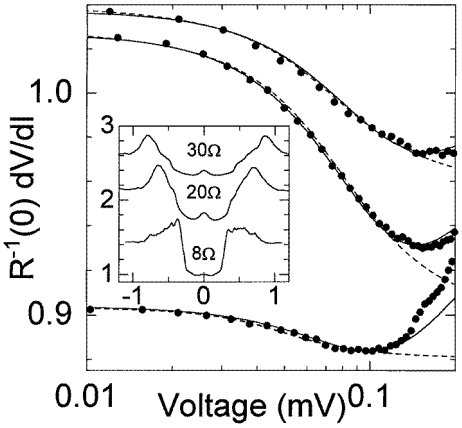

Figure 6. The reduced dV/dI versus V around zero bias along the a-direction at $T \leqslant 0.1$ K (points), fitted by the modified BTK model (solid lines, equation (3)) and by the Kondo model (dashed lines, equation (5)). The fitting parameters Δ, Z, and Γ for the solid lines are (from top to bottom) 0.08 meV, 0.87, and 0.1 meV; 0.09 meV, 0.84, and 0.09 meV; and 0.09 meV, 0.52, and 0.09 meV. The fitting parameters β, V_k, and S for the dashed lines are (from top to bottom) 0.043, 0.075 mV, and 0.075; 0.068, 0.08 mV, and 0.07; and 0.012, 0.05 mV, and 0.05. The inset shows the same dV/dI curves on a larger voltage scale, and the zero-bias resistance. The curves are offset vertically for clarity.

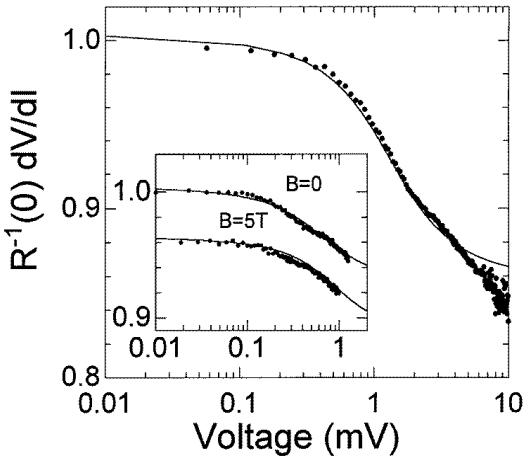

Figure 7. The reduced dV/dI versus V along the c-direction at $T \leqslant 0.1$ K and $B = 0$ for a PC with $R(0) = 9.9$ kΩ (points), fitted using equation (5) (solid lines). The fitting parameters are $\beta = 0.075$, $V_k = 1.3$ mV, and $S = 0.135$. The inset shows another PC along the a-direction with $R(0) = 260\ \Omega$ at $T \leqslant 0.1$ K. The fitting parameters β, V_k, and S are: 0.04, 0.65 mV, and 0.21 at $B = 0$; and 0.04, 0.9 mV, and 0.17 at $B = 5$ T. The curves are offset vertically for clarity.

analogously to the method in reference [21] for PC with the HF superconductor UPt_3. The free parameters were the SC gap Δ, the barrier strength Z, and the broadening parameter Γ. For the Kondo fit, we used the Hamann expression for the temperature dependence of the resistivity [22] like in reference [23]. Here the temperature T is simply replaced by the

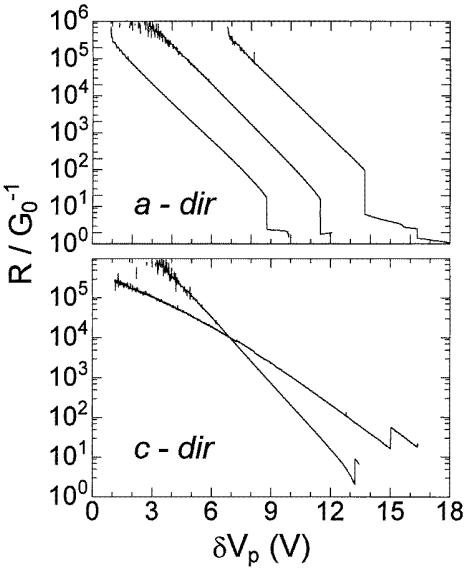

Figure 8. The reduced MCB resistance R in units of G_0^{-1} versus the relative change of the piezo-voltage δV_p at $T \leqslant 0.1$ K for successive piezo-voltage sweeps along the a- (top) and the c- (bottom) directions. The bias voltage was 0.1 V in both cases.

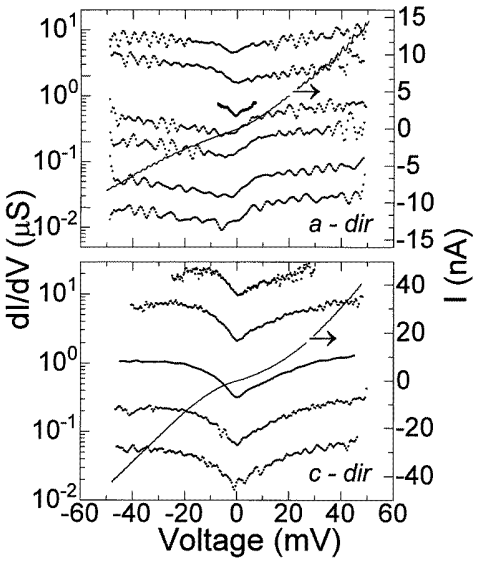

Figure 9. The numerical derivatives (solid points) of the I–V curves at $T \leqslant 0.1$ K for the a-direction and the c-direction. The solid lines show typical I–V curves.

voltage V to obtain

$$\mathrm{d}V/\mathrm{d}I(V) \propto 1 + \beta \left\{ 1 - \frac{\ln(V/V_K)}{\sqrt{\ln^2(V/V_K) + \pi^2 S(S+1)}} \right\} \tag{5}$$

with $V_K \simeq k_B T_K/e$ corresponding to the Kondo temperature T_K, S the local moment of the magnetic ion, and β a scaling coefficient. Figure 6 shows that both models yield a good description with reasonable fitting parameters: Δ is about 0.08–0.09 meV, $Z = 0.5$–0.8, and $\Gamma = 0.09$–1 meV, while the Kondo temperature is about 0.6–1 K, and the local moment (probably that of uranium) is only about 0.1, possibly because of screening by the conduction electron.

4.3. High-ohmic contacts

At contact resistances above about 1 kΩ, no SC features are resolvable. The $\mathrm{d}V/\mathrm{d}I$ characteristics show a broad maximum at $V = 0$ of width ranging from 2 to 4 mV (figure 7). Usually $\mathrm{d}^2V/\mathrm{d}I^2$ is negative in the voltage range investigated, ±30 mV. An estimate of the Kondo temperature according to equation (5) yields $T_K \approx 7$–15 K and $S \simeq 0.1$–0.2. Magnetic fields up to 5 T only broaden the curves (figure 7, inset). This is consistent with the rather large Kondo fields of order $k_B T_K/\mu_B \approx 10$–22 T. It was difficult to measure the same PC continuously in the field, because the contacts become unstable due to the large magnetostriction of URu_2Si_2 [24].

These high-ohmic contacts, as well as most contacts with $R_N > 100$ Ω, were unstable on changing the temperature, because of the large thermal expansion of URu_2Si_2. This

hinders both the determination of the PC diameter d from $R_{PC}(T)$ and the investigation of the temperature dependences of the $\mathrm{d}V/\mathrm{d}I(V)$ curves.

4.4. Vacuum-tunnelling contacts

The experimental verification of the vacuum-tunnelling regime is the observing of an exponential dependence of the tunnelling current or the MCB resistance on the piezo-voltage V_p. We did indeed obtain such a dependence for several single-crystal junctions (figure 8). A one-decade change of the resistance corresponds to a change of approximately 2 V in the piezo-voltage, close to our experimental results on aluminium [7]. With polycrystalline URu_2Si_2 samples, we failed to get a good exponential behaviour, and the $R(V_p)$ curves showed a lot of noise. Qualitatively, the $R(V_p)$ dependences are the same for both crystallographic directions. (After reaching metallic contact in the c-direction, the resistance often jumped upward. This might be caused by the rearrangement of atoms being different along the two crystallographic directions.) The resistance after the drop to metallic contact was usually between 10 and 50 kΩ, near $R_0 = G_0^{-1} = h/2e^2 = 12.9$ kΩ, where G_0 is the conductance quantum unit, the value expected for simple metals [8].

We have measured I–V characteristics of the vacuum-tunnel junctions in the 0.2–100 MΩ range. They were numerically differentiated to search for SC structure (see figure 9). One should expect a minimum in $\mathrm{d}I/\mathrm{d}V$, and a gap of width $4\Delta_0 \simeq 7.04\,k_\mathrm{B}T_c \simeq 0.8$ mV. But such structures could not be resolved. Instead, a broad and shallow minimum (that was more pronounced in the c-direction) with a width of 10–20 mV could be seen. This width increases slightly with increasing MCB resistance. We do not know whether this minimum is related to superconductivity or to antiferromagnetism. Measuring the temperature dependence of the $\mathrm{d}I/\mathrm{d}V$ minimum was impossible, because of thermal-expansion effects. They change the MCB resistance by several orders of magnitude when the temperature is increased above T_c, and probably vary the lateral position of the junction. In contrast to our results, STM experiments [25, 26] showed a pronounced minimum in $\mathrm{d}I/\mathrm{d}V$ along the ab-plane.

Finally, we have measured the temperature dependence of the tunnelling current at constant bias and piezo-voltage. $I(T)$ changes by orders of magnitude. Since $I(T) \sim \exp\{-a\ell(T)\}$ [2], ℓ being the distance between the electrodes and a a constant, the logarithmic derivative of the current versus temperature yields directly the thermal-expansion coefficient $\alpha = \Lambda^{-1}\,\mathrm{d}\Lambda/\mathrm{d}T = -\Lambda^{-1}\,\mathrm{d}\ell/\mathrm{d}T \sim \Lambda^{-1}\mathrm{d}\{\log(I)\}/\mathrm{d}T$. Here $\Lambda \simeq 1$ mm is the free length of the sample. These data plotted in figure 10 agree well with an anisotropic bulk thermal-expansion coefficient of URu_2Si_2 single crystals [24], if the temperature is normalized to T^*, the temperature at which α changes sign. The different $T^* \simeq T_c$ probably result from differences in the sample quality.

5. Discussion

The relationship between the drop of the PC resistance in the SC state and the lateral size of the junctions over a wide resistance range (figure 2) provides strong evidence that the observed SC features mainly result from the Maxwell term of R_{PC}. Superconductivity can be suppressed in the contact region by local heating at a rate $eV = 3.63\,k_\mathrm{B}T$ [17] if the contact is in the thermal regime. This relation almost coincides with the well-known BCS equation $2\Delta_0 = 3.52\,k_\mathrm{B}T_c$. Additionally, the similarity of the temperature dependences of $\Delta(T)$ and of the critical voltage $V_c(T)$ according equation (4) (see figure 5(c)) might lead one to misinterpret the thermal-regime anomalies of $\mathrm{d}V/\mathrm{d}I$ as spectroscopic ballistic ones,

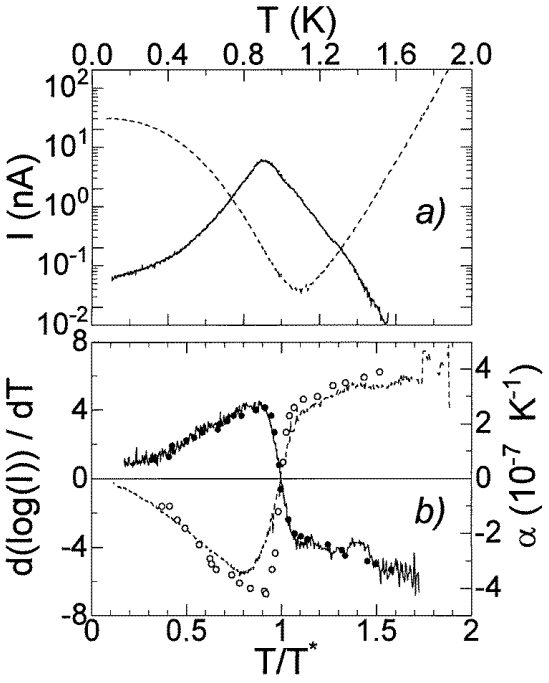

Figure 10. (a) The tunnelling current I versus temperature T at constant piezo-voltage and bias voltage 0.1 V along the c- (solid line) and a- (dashed line) directions. (b) The logarithmic derivative of the $I(T)$ curves versus the reduced temperature T/T^*. Here T^* is 1.1 K for the a-direction and 0.91 K for the c-direction. Open and closed circles show the temperature dependence of the thermal-expansion coefficients from reference [24] for two directions with $T^* = 1.2$ K.

and to an incorrect determination of the SC order parameter and its spatial and temperature dependence.

The absence of Josephson oscillations of the critical current of low-ohmic contacts that have zero resistance at $V = 0$ may be due to the ballistic contribution to the resistance being extremely small. For contacts with $R \leqslant 0.2\ \Omega$ ($d \geqslant 1\ \mu$m) Sharvin's resistance is less than 1/100 of the total normal-state resistance, assuming the bulk value of the residual resistivity and a typical metallic electron density of the URu_2Si_2 [1]. This means that most of the critical current observed is related to the suppression of Maxwell's resistance in the SC state.

After fully breaking and readjusting the junction, no supercurrent could be found, even for low-ohmic contacts. Those contacts behave as S–N–S junctions with a thick normal (N) layer. For S–c–S contacts the Josephson effect (JE) is expected to survive as long as the width of the region with the reduced order parameter (e.g. the normal layer) is less than 3ξ [27]. Thus, already a thin (about 30 nm) normal layer may explain the absence of Josephson coupling. This layer, which is probably of magnetic origin, also hinders the observation of SC features by means of vacuum tunnelling that 'senses' the topmost atomic layer.

AR at the S–N interfaces with this layer could produce a double-minimum structure, as shown in figure 6. Alternatively, Kondo scattering at localized magnetic moments (i.e. uranium) in the contact region may also yield a maximum at zero bias, and create rather similar features. To distinguish between AR and Kondo scattering at low-ohmic contacts is

not straightforward, because both models yield reasonable fitting parameters. Note that the zero-bias maximum becomes the most pronounced feature for MCB with resistance above a few hundred ohms (see figure 7), when the SC structure is fully depressed. This maximum is very probably of magnetic nature.

In the tunnelling regime the current is proportional to $\exp(-2\ell\sqrt{2m\phi}/\hbar)$ [2]. Here ϕ is the metallic workfunction and m the electron mass. The slope of $\ln(I)$ versus $\ln(\ell)$ defines the product $m\phi$. Experimentally, ℓ is proportional to the piezo-voltage V_p; therefore ℓ can be substituted for with V_p. We observed qualitatively the same slope of $\ln(I)$ versus $\ln(V_p)$ for Al MCB [7]. And if we assume that URu_2Si_2 has the same workfunction as most metals and alloys [28], then the tunnelling charge carriers of URu_2Si_2 would have a nearly free-electron mass. Slight differences in the slope (see figure 10) even for the same MCB may result from the electrodes moving not perfectly normally to surface of the junction.

On the other hand the transition from tunnelling to metallic contact (a drop from a high resistance of 0.2–1 MΩ to 10–50 kΩ) of our URu_2Si_2 MCB takes place in the same resistance range as for simple metals, contrary to the case for semimetals [29]. This indicates that the charge carriers of URu_2Si_2 have a typical metallic Fermi wavelength, and a carrier density of 10^{22}–10^{23} cm^{-3}.

Our tunnelling measurements do not show the presence of 'heavy' electrons or a small effective Fermi wavenumber. Further experiments on the tunnelling–metallic transition, and the search for the quantization of conductance are much needed.

6. Conclusion

We investigated mechanically controllable break junctions of the HF superconductor URu_2Si_2. Thermal transport and the freezing out of normal scattering processes contribute considerably to the SC signal, while no clear-cut evidence for a JE and AR could be found. The spatial as well as the temperature dependence of the SC order parameter (energy gap) may still be recovered from the spectra of those contacts if one establishes what the regime of electron transport across the junction is. This requires one to distinguish between a number of processes involved, mainly local heating at a rate of approximately $k_BT = eV/3.63$, and the destruction of SC by a high current density or by the self-magnetic field of the current through the junction. For junctions in the intermediate regime between metallic conduction and vacuum tunnelling, a study of conductance quantization versus lateral contact dimension would yield information about the Fermi wavelength. For the vacuum-tunnelling regime the main question still is that of whether it is really possible to observe intrinsic properties of the HF compounds.

Acknowledgments

We are grateful to R Häußler for allowing us to use his fitting program for the modified BTK model. YuGN thanks the Institut für Festkörperphysik, Technische Hochschule Darmstadt, for hospitality and I K Yanson for encouragement. This work was supported in part by SFB 252 Darmstadt/Frankfurt/Mainz and the German BMBF Grant No 13N6608/1.

References

[1] Grewe N and Steglich F 1991 *Handbook on the Physics and Chemistry of Rare Earths* vol 14, ed K A Gschneidner Jr and L Eyring (Amsterdam: North-Holland) p 343

[2] Wolf E L 1985 *Principles of Electron Tunneling Spectroscopy* (New York: Oxford University Press) p 125

[3] Blonder G E, Tinkham M and Klapwijk T M 1982 *Phys. Rev.* **25** 4515
[4] Muller C J, van Ruitenbeek J M and de Jongh L J 1992 *Physica* C **191** 485
[5] Mydosh J A 1987 *Phys. Scr.* **19** 260
[6] Gloos K, Anders F B, Buschinger B and Geibel C 1997 *Physica* B **230–232** 391
[7] Gloos K 1997 at press
[8] Krans J M, Muller C J, Yanson I K, Govaert T C M, Hesper R and van Ruitenbeek J M 1993 *Phys. Rev.* B **48** 14 721
[9] Wexler A 1966 *Proc. Phys. Soc.* **89** 927
[10] Akimenko A I, Verkin A B, Ponomarenko N M and Yanson I K 1982 *Sov. J. Low Temp. Phys.* **8** 130
[11] Srikanth H and Raychaudhuri A K 1992 *Physica* C **190** 229
Pleceník A, Grajcar M, Beňačka Š, Seidel P and Pfuch A 1994 *Phys. Rev.* B **49** 10 016
[12] Kulik I O and Omelyanchouk A N 1975 *JETP Lett.* **21** 96
Kulik I O and Omelyanchouk A N 1977 *Sov. J. Low Temp. Phys.* **3** 459
Kulik I O and Omelyanchouk A N 1978 *Sov. J. Low Temp. Phys.* **4** 142
[13] Van Harlingen D J 1995 *Rev. Mod. Phys.* **67** 515
[14] Gloos K, Kim S J and Stewart G R 1996 *J. Low Temp. Phys.* **102** 325
Gloos K, Geibel C, Müller-Reisener R and Schank C 1996 *Physica* B **218** 169
Gloos K, Anders F B, Buschinger B, Geibel C, Heuser K, Järling F, Kim S J, Klemens R, Müller-Reisener R, Schank C and Stewart G R 1996 *J. Low Temp. Phys.* **105** 37
[15] Naidyuk Yu G and Kvitnitskaya O E 1991 *Sov. J. Low Temp. Phys.* **17** 439
Häußler R, Goll G, Naidyuk Yu G and von Löhneysen H 1996 *Physica* B **218** 197
[16] Naidyuk Yu G, Nowack A, Yanson I K and Chubov P N 1991 *Sov. J. Low Temp. Phys.* **17** 1170
Nowack A, Naidyuk Yu G, Chubov P N, Yanson I K and Menovsky A A 1992 *Z. Phys.* B **88** 295
[17] Kulik I O 1992 *Sov. J. Low Temp. Phys.* **18** 450
[18] de Gennes P G 1966 *Superconductivity of Metals and Alloys* (New York: Benjamin)
[19] Naidyuk Yu G, von Löhneysen H, Goll G, Yanson I K and Menovsky A A 1996 *Europhys. Lett.* **33** 557
[20] Yanson I K, Fisun V V, Hesper R, Khotkevich A V, Krans J M, Mydosh J A and van Ruitenbeek J M 1995 *Phys. Rev. Lett.* **74** 302
[21] Naidyuk Yu G, von Löhneysen H, Goll G, Paschke C, Yanson I K and Menovsky A A 1996 *Physica* B **218** 161
[22] Hamann D R 1967 *Phys. Rev.* **158** 570
[23] Jansen A G M, van Gelder A P and Wyder P 1980 *J. Phys. C: Solid State Phys.* **13** 6073
[24] van Dijk N H, de Visser A, Franse J J M and Menovsky A A 1995 *Physica* B **206** 583
[25] Aliev A, Agraït N, Vieira S, Villar R, Kovachik V, Moshchalkov V V, Pryadun V V, Alekseevskii N E and Mitin A V 1991 *J. Low Temp. Phys.* **85** 359
[26] Aarts J, Volodin A P, Menovsky A A, Nieuwenhuys C J and Mydosh J A 1994 *Europhys. Lett.* **26** 203
[27] Licharev K K 1985 *Introduction to the Dynamics of Josephson Junctions* (Moscow: Nauka) (in Russian)
[28] Riviere J C 1969 *Solid State Surface Science* vol 1, ed M Green (New York: Dekker) section 4
[29] Krans J M and van Ruitenbeek J M 1994 *Phys. Rev.* B **50** 17 659